

# Three-Channel Correlation Analysis: A New Technique to Measure Instrumental Noise of Digitizers and Seismic Sensors

by Reinoud Sleeman, Arie van Wettum, and Jeannot Trampert

**Abstract** This article describes a new method to estimate (1) the self-noise as a function of frequency of three-channel, linear systems and (2) the relative transfer functions between the channels, based on correlation analysis of recordings from a common, coherent input signal. We give expressions for a three-channel model in terms of power spectral densities. The method is robust, compared with the conventional two-channel approach, as both the self-noise and the relative transfer functions are extracted from the measurements only and do not require *a priori* information about the transfer function of each channel. We use this technique to measure and model the self-noise of digitizers and to identify the frequency range in which the digitizer can be used without precaution. As a consequence the method also reveals under which conditions the interpretation of data may be biased by the recording system. We apply the technique to a Quanterra Q4120 datalogger and to a Network of Autonomously Recording Seismographs (NARS) datalogger. At a sampling rate of 20 samples/sec, the noise of the Q4120 digitizer is modeled by superposition of a flat, 23.6-bit spectrum and a 24.7-bit spectrum with  $1/f^{1.55}$  noise. For the NARS datalogger the noise level is modeled by superposition of a 20.8-bit flat spectrum and a 23.0-bit spectrum with  $1/f^{1.0}$  noise. The measured gain ratios between the digitizers in the Q4120 datalogger, smoothed over a tenth of a decade between 0.01 Hz and 8 Hz for data sampled with 20 samples/sec, are within 1.6% (or 0.14 dB) of the values given by the manufacturer. Finally, we show an example of seismic background noise observations at station HGN as recorded by both an STS-1 and a STS-2 sensor. Between 0.01 and 0.001 Hz the vertical STS-2 noise levels are 10–15 dB above the STS-1 observations. The Quanterra Q4120 digitizer noise model enables us to exclude the contribution of the digitizer noise to be responsible for this difference.

## Introduction

Broadband (BB) and very broadband (VBB) seismic sensors are used in global, regional, and even local seismological studies because of their wide-frequency response, low-self-noise level, and large dynamic range. Typical bandwidths (all instrumental specifications in this introduction are taken from the manufacturers) for VBB sensors are from around 360 sec to 5 Hz (KS54000) or to 10 Hz (STS-1, CMG-1T). For BB sensors the bandwidths range between 120 sec and 50 Hz (STS-2, KS-2000, CMG-3T) and 40 sec and 50 Hz (Trillium). These bandwidths specify the frequency ranges in which the instruments have a (more or less) flat response to ground velocity. The self-noise of these sensors is typically close to the U.S. Geological Survey (USGS) New Low Noise Model (NLNM) (Peterson, 1993) over large frequency bands (CMG-1T, about 300 sec to 20 Hz; STS-1,  $10^5$  sec to about 2.5 Hz) or smaller bands (EP-300, 20 sec to 5 Hz; CMG-40T, 10 sec to 1 Hz). In some frequency bands the output of the sensors can thus reflect, at most sites,

the Earth noise in the absence of seismicity, and the seismic records will not be influenced by the instrumental self-noise. At longer periods (above 200 sec) the NLNM is essentially coincident with the self-noise of the STS-1 (Wielandt, 2002a), whereas current other broadband sensors show instrumental noise above the NLNM (Widmer-Schmidrig, 2003). To capture the large dynamic range of seismic signals from ambient Earth noise to earthquakes as large as magnitude  $M_w$  9.5 at 90° epicentral distance (Incorporated Research Institutions for Seismology [IRIS], 2003) the sensors are designed to provide a large dynamic range (Wielandt and Steim, 1986). Broadband seismometers usually are of a force balance feedback design and have dynamic ranges up to roughly 160 dB.

Current high-resolution data-acquisition systems are specifically designed to cover a large part of the bandwidth and dynamic range of the sensors. These digitizers are based on delta-sigma modulators (e.g., Candy and Temes, 1992),

which decrease the quantization errors at lower frequencies at the price of increased quantization errors at high frequencies. By using a high initial sampling rate (in the order of tens of kilohertz) the quantization error will decrease in the frequency range of seismic interest (e.g.,  $f < 200$  Hz). Through the use of these “noise-shaping” digitizers the dynamic range of seismic dataloggers, often expressed by a single number representing the ratio of the largest to the smallest signal that can be recorded (Bennett, 1948), may range up to about 145 dB. The representation of the behavior of a digitizer by a single number is convenient but does not reflect the true dynamic behavior of the digitizer as function of the frequency. First, the dynamic range of the digitizer is not a static value but depends on the sampling rate and the frequency. The noise-shaping effect of the oversampled delta-sigma digitizers results in a larger dynamic range at lower sample frequencies. Second, at lower frequencies (e.g.,  $f < 1$  Hz) the self-noise of the digitizers will increase like in any other active electronic component. This so-called  $1/f$  type noise may therefore decrease the dynamic range at lower frequencies. Also, the generation of additional noise over the total frequency band due to nonlinearity or distortion in the system may decrease the dynamic behavior.

The choice of a particular type of sensor and digitizer is usually driven by constraints on the frequency band and the amplitude range of interest. Not only for selection criteria it is important to have this type of information available, but also in the process of data interpretation. For example, the presence of  $1/f$  noise may bias the data analysis and the resolution of the digitizer (in the frequency band of interest) determines the minimum amplitude difference that can be resolved properly. Today’s high dynamic range digitizers are specifically designed to match the present generation of seismic sensors. The use and development of other sensors, like superconducting gravimeters (e.g., Freybourger *et al.*, 1997; Rosat *et al.*, 2003; Warburton, 2004) showing lower self-noise than current devices, may put additional demands on the dynamic range and resolution of digitizers. The noise reduction in vertical seismic recordings below a few millihertz with local barometric pressure correction (Roult and Crawford, 2000) permits the achievement of noise levels well below the NLNM (Zürn and Widmer, 1995; Beauvin *et al.*, 1996; Widmer-Schnidrig, 2003), which means that the NLNM may need some minor revision. Also, the analysis technique by Berger *et al.* (2004) applied to recordings from the Global Seismographic Network (GSN) shows noise levels below the NLNM. The interpretation of such low-noise data would only make sense if the noise level of the data is above the noise levels of sensor and digitizer at these low frequencies (Clinton and Heaton, 2002).

The main purpose of this article is to present and use a robust technique to measure and model digitizer noise and to identify the frequency range in which the digitizer can be used without precaution. As a consequence the method will also reveal under which conditions the interpretation of noise records may be biased by the recording system. The first

section describes the relationship between the dynamic range of a digitizer, the number of quantization levels (bits), the clip level, and the sampling rate. This relationship will be useful in modeling the behavior of the digitizer. The technique to compute the frequency-dependent noise level of three-channel digitizers, based on the Modified Noise Power Ratio test (McDonald, 1994), is described in the next section. The method in this article uses three digitizers with a common broadband input. Coherency analysis of the output recordings provides the power of the noise (for each channel) as function of frequency. In the next section this technique is applied to both a Quanterra Q4120 datalogger ([www.kinometrics.com](http://www.kinometrics.com)) and a NARS datalogger ([www.geo.uu.nl/Research/Seismology/Logger](http://www.geo.uu.nl/Research/Seismology/Logger)) to reveal the  $1/f$  behavior and the resolution of the digitizers. For both dataloggers a simple model is presented to approximate the power spectral density of the digitizer noise. In the last section we show seismic background noise observations at station HGN (<http://www.orefeus-eu.org/working.groups/wg1/station.book/HGN/HGN.html>) as recorded by an STS-1 and a STS-2 sensor in the same vault. After correcting the recorded data for the instrument response, the vertical STS-2 recordings have noise levels of 10–15 dB above the STS-1 recordings in the frequency range 0.01–0.001 Hz. Having the Quanterra Q4120 digitizer noise model we can exclude the contribution of the digitizer noise to be responsible for this difference.

### Dynamic Range of a Digitizer

The quantization process of a digitizer can be modeled as the addition of random noise  $e$  to the input sample  $x$ :

$$e = q(x) - x, \quad (1)$$

where  $q(x)$  is the digitized value of  $x$ . To describe the basic properties of such a digitizer it is often assumed that the quantization noise  $e$  is signal-independent, uniformly distributed, and uncorrelated (white) noise. Although the white-noise assumption may be violated in oversampled digitizers (Gray, 1990), the assumption is more realistic when the signal becomes more complicated. For complicated signals the correlation between the signal and the quantization error decreases, and the error becomes uncorrelated (Bennett, 1948). The uniform white quantization noise assumption is made often when there is no *a priori* knowledge of the statistical behavior of the digitizer input. Assuming that the quantization error time series  $e$  is white noise and has a uniform probability density function  $p(e) = 1/\Delta$  within the interval  $[-\Delta/2, \Delta/2]$ , where  $\Delta$  is the quantization interval, the variance of the error is given by:

$$\begin{aligned} e_{\text{rms}}^2 &= \int_{-\infty}^{\infty} [q(x) - x]^2 p(e) de \\ &= \frac{1}{\Delta} \int_{-\Delta/2}^{\Delta/2} e^2 de = \frac{\Delta^2}{12}. \quad (2) \end{aligned}$$

Bennett (1948) used this result to estimate the magnitude of the quantization noise with respect to a full-load sine wave, which is also called the dynamic range or signal-to-noise ratio (SNR):

$$\text{SNR} = 10 \cdot \log \left( \frac{s_{\text{rms}}^2}{e_{\text{rms}}^2} \right) \quad [\text{dB}], \quad (3)$$

where  $s_{\text{rms}}^2$  is the mean square of the full-scale sine wave. For a sine wave with amplitude  $A$  the effective amplitude  $s_{\text{rms}}$  is given by  $A/\sqrt{2}$ . The quantization interval  $\Delta$ , also called the least-significant bit (LSB), and the full-scale input amplitude  $2A$  determine the number of quantization levels (Oppenheim and Schaffer, 1998, p. 205):

$$\frac{2A}{\Delta} = 2^n, \quad (4)$$

in which  $n$  is known as the number of bits of the digitizer. Using equations (2) and (4) the dynamic range in equation (3) can be expressed by the number of bits of the digitizer:

$$\text{SNR} = 10 \cdot \log \left( \frac{A^2/2}{\Delta^2/12} \right) = 1.76 + n \cdot 6.02 \quad [\text{dB}]. \quad (5)$$

This expression shows that the dynamic range increases by about 6 dB per digitizer bit.

A more realistic way to specify the dynamic range of a digitizer is as a function of frequency. This is because an inherent characteristic of digitizers based on solid-state devices (like semiconductors) or photoelectric devices is the presence of  $1/f$  type noise, noise whose power spectral density is inversely proportional to frequency. Also the saturation level of digitizers is, in general, frequency dependent. In this article, however, we assume that the clip level remains constant over the frequency band of interest so that the frequency dependence of the dynamic range is only determined by the quantization noise. In an ideal digitizer (assuming white quantization noise) the quantization noise power (equation 2) is uniformly distributed between dc and the Nyquist frequency  $f_N$  (Aki and Richards, 1980, pp. 597–599). Because the noise power is independent of the sampling rate (Fig. 1), the (one-sided) power spectral density,  $\text{PSD}_{\text{noise}}(f)$ , of the quantization process is:

$$\text{PSD}_{\text{noise}}(f) = \frac{\Delta^2}{12} \cdot \frac{1}{f_N}. \quad (6)$$

Therefore, for higher sampling rates the noise power is spread over a wider range of frequencies (Oppenheim and Schaffer, 1998, p. 204), and this decreases the noise PSD in the band of interest as indicated schematically by levels P1 and P2 in Figure 1. Substituting equation (4) in equation (6) gives:

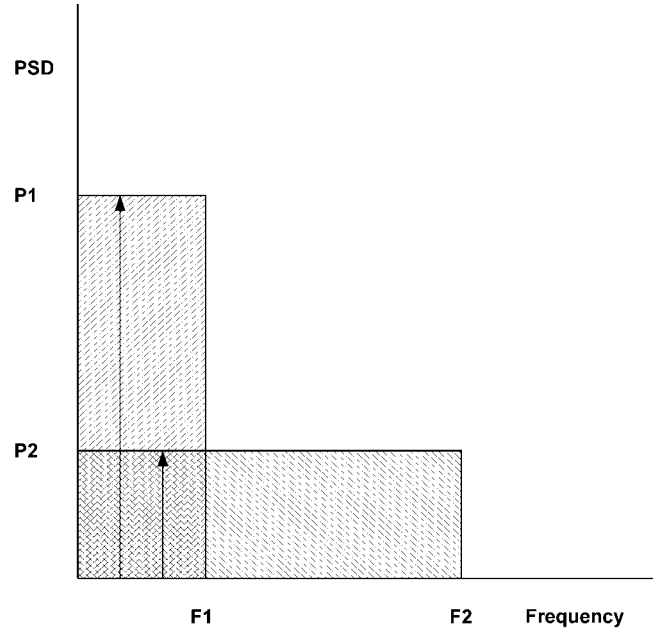


Figure 1. One-sided power spectral density (PSD) levels (P1 and P2) for an ideal quantization process using two different sampling rates with corresponding Nyquist frequencies  $F1$  and  $F2$ . The area of the rectangle bounded by frequency  $F1$  and PSD level  $P1$  equals the area bounded by  $F2$  and  $P2$ . Both areas are equal to the quantization noise power in equation (2).

$$\text{PSD}_{\text{noise}}(f) = \left( \frac{2A}{2^n} \right)^2 \cdot \frac{1}{12 \cdot f_N} = \left( \frac{2A}{2^n} \right)^2 \cdot \frac{T}{6}, \quad (7)$$

which relates the noise level  $\text{PSD}_{\text{noise}}(f)$  of the digitizer to the sampling interval  $T$  ( $T = 1/(2f_N)$ ), the number of quantization levels (or bits)  $n$  and the full-scale input  $2A$ .

### Dynamic Range Measurement

The dynamic range of a data-acquisition system quantifies the ratio of the largest number (clip level) that can be represented by the system and the quantization error (self-noise). A fairly simple way to measure the self-noise is to short-circuit the input of the digitizer and record the output. In this article the input connectors are terminated with 50-ohm resistors, to simulate the output impedance of an active seismic sensor. The clip level could be measured using a sine wave generator, but the clip levels used in this report are taken from the manufacturers specifications.

There are several ways to calculate and represent the dynamic range of a system (Hutt, 1990). One way is to calculate the ratio of the maximum peak amplitude of the recorded self-noise and the clip level. A more common way is to measure the dynamic range in a specified frequency band, and express this by a single number as the ratio of the root mean square (rms) of the noise and the rms of a full-scale sine wave:

$$\text{SNR} = 20 \cdot \log \left( \frac{\text{rms full-scale sine}}{\text{rms noise}} \right), \quad (8)$$

where the rms of the noise is measured in the specified bandwidth. This number is often used by vendors to quantify the dynamic range of their systems. Finally, the dynamic range can be represented in a graph as a function of the frequency and is obtained by measuring the PSD of the recorded noise and applying equation (7). This way of representing reflects in a more realistic way the dynamic behavior of the digitizer and will also reveal the  $1/f$  type noise.

The PSDs shown in this article are estimated by using Welch's averaged periodogram method (Welch, 1967). In this method a time series is divided into a number of overlapping sections of data. In each section we remove the mean, apply a taper on the data, and calculate the power spectrum by taking the square of the discrete Fourier transform of the tapered data. Finally, an estimate of the PSD is obtained by averaging the power spectra over the number of sections. The windows are tapered with a normalized Hanning window and have an overlap of 50%. All PSDs are calculated by using the definition from engineering where the power is attributed to positive frequencies only. This so-called one-sided PSD (as opposed to two-sided PSD in which power is attributed to positive and negative frequencies [Press *et al.*, 1988, pp. 401–402]) was used by Peterson (1993) to construct the NLNM. Our results are compared with the NLNM.

The short-circuited input test does not measure the non-linearity or distortion of the system. On the other hand, delta-sigma modulators may produce periodic oscillations when there is no input signal (Baker, 1997). One way to reduce this idle tone problem is to introduce a small offset voltage to the input signal. Our results do not show idle tones in the short-circuited input tests. Nonlinear behavior of delta-sigma modulator electronics may be introduced with large-amplitude input signals and generate additional noise that depends on the signal level. This additional signal-generated noise may therefore decrease the dynamic range at large-input signals. The effect of this type of generated noise can be measured by feeding multiple digitizers with a common, large, and well-defined signal. Historically, the linearity of a seismic system has been measured in a two-tone test (Steim, 1986), in which the system is driven by two sine waves with nearly identical frequencies (Hutt, 1990). In this report, however, we focus on the behavior of the self-noise only, in the presence of a common input signal. In this report the common input for the digitizers was the output of the vertical component of a STS-2 sensor. The sensor was located at a site at which the ratio between the seismic background noise and the estimated digitizer noise was roughly about 40 dB over a large frequency range. After removing the coherent signal between the digitizer outputs, each digitizer output will reflect its self-noise.

To estimate the self-noise of digitizers we developed a

new technique using coherency analysis. In the conventional approach to estimate the self-noise of linear systems, two systems are used and fed by a common, coherent input signal. This technique has been used in many studies to calibrate seismometers (e.g., Berger *et al.*, 1979; Holcomb, 1989; Pavlis and Vernon, 1994), in which two seismometers are placed close together so that it can be assumed that they record the same ground motion. The mathematical solution of such a system is very simple, but the practical application is limited because the method assumes that one of the pairs of sensors has an accurate known frequency response. Small errors in the transfer functions (or gains) in the two linear systems will cause relatively large errors in the calculated noise levels (Holcomb, 1989). Our approach uses three linear systems that are also fed by a common input signal. The following mathematical description of the model shows the advantages of this approach as opposed to the conventional two-channel approach.

The output  $y_i$  of digitizer  $i$  can be written as the convolution of the input signal  $x$  with the digitizer's impulse response  $h_i$ , plus the internal noise  $n_i$ :

$$y_i = x \otimes h_i + n_i, \quad (9)$$

where  $i = 1,2,3$  and  $\otimes$  denotes convolution. Some two-channel models add noise to the input signal (Holcomb, 1990), but for the purpose of self-noise it is appropriate to add transfer-function-independent noise. For analog systems there is no difference in this approach as the relation between the noise at the output and the noise at the input is defined by the (well enough known) transfer function. For digitizers one can expect slightly different statistical properties between the quantized output noise and the (analog) input noise. Equation (9) translates in the frequency domain to:

$$Y_i = X \cdot H_i + N_i, \quad (10)$$

where  $Y_i$ ,  $X$ ,  $H_i$ , and  $N_i$  represent the Fourier transforms of  $y_i$ ,  $x$ ,  $h_i$ , and  $n_i$ . We assume that (1) the internal noise between two channels is uncorrelated and (2) the internal noise  $n_i$  and the input signal  $x$  are uncorrelated (see above). Then, the cross-power spectra  $P_{ij}$  (Oppenheim and Schaffer, 1998) between digitizers  $i$  and  $j$  can be written as:

$$P_{ij} = Y_i \cdot Y_j^* = P_{xx} \cdot H_i \cdot H_j^* + N_{ij}, \quad (11)$$

where  $*$  denotes complex conjugation,  $P_{xx} = X \cdot X^*$  is the autopower spectrum of the common input signal, and  $N_{ij}$  is the cross-power spectrum between  $n_i$  and  $n_j$ . For  $i \neq j$  the noise cross-power spectra  $N_{ij}$  is assumed to be zero, so that:

$$\frac{P_{ji}}{P_{ki}} = \frac{H_j}{H_k}, \quad (12)$$

with  $i, j, k = 1,2,3$  and  $i \neq j \neq k$ . This equation reveals that

the ratio between the transfer functions of digitizer  $j$  and  $k$  can be estimated solely by the ratio of the cross-power spectra between channels  $j$  and  $i$  and the cross-power spectra between channels  $k$  and  $i$ . Taking the ratio between autospectra  $P_{ii}$  and cross-spectra  $P_{ji}$  gives:

$$\frac{P_{ii}}{P_{ji}} = \frac{H_i}{H_j} + \frac{N_{ii}}{P_{ji}}. \quad (13)$$

Note that the index  $ii$  does not mean summation. Substituting equation (12) in equation (13) gives the expression for the noise autopower spectrum for digitizer  $i$ :

$$N_{ii} = P_{ii} - P_{ji} \cdot \frac{P_{ik}}{P_{jk}}, \quad (14)$$

with  $i, j, k = 1, 2, 3$  and  $i \neq j \neq k$ . This equation expresses the power spectra of the system noise, only in terms of the cross-power spectra and autopower spectra of the recordings of the three digitizers connected to the same (analog) input signal. The mathematical description of the three-channel linear system model shows that we can estimate, solely from the output recordings, (1) the ratio of the transfer functions between the channels and (2) the noise spectrum for each channel. We do not need to know the transfer functions, or its accuracy as is required in the two-channel model.

### Tests and Results

First the self-noise of three digitizer channels in a Quanterra Q4120 (S/N 2000.036) is recorded with short-circuited input connectors. The input connectors are terminated with 50 ohm resistors to simulate the output impedance of an active seismic sensor, and during 24 hours the self-noise was recorded with sampling rates of 1, 20, and 100 samples/sec. The effective amplitude (rms) of the noise is calculated in the frequency band between 0.01 Hz and 80% of the Nyquist frequency. The latter value is taken to discard the steep cut-off effect of the finite impulse response (FIR) filter above 80% of the Nyquist frequency. Table 1 gives the dynamic range of the three tested digitizers, determined by using equation (8). The three digitizers have a dynamic range of more than 140 dB for sampling rates up to 100 samples/sec, and as expected the dynamic range increases at lower sampling rates.

To extract the dynamic range as a function of frequency the short-circuited time series are processed using equation (14) on recordings of 2 hr for the 100 samples/sec data streams and 4 hr for 20 samples/sec data (Fig. 2). For frequencies above (roughly) 1 Hz the noise is flat and the PSD does not vary significantly with frequency. However below 1 Hz the  $1/f$  type of noise dominates and the dynamic range decreases at lower frequencies. The horizontal lines show theoretical PSD levels for 22-, 23-, 24-, and 25-bit digitizers as derived from equation (7). The corresponding values for

Table 1

Single Number Representation of the Dynamic Range (SNR) of Three Digitizers in the Quanterra Q4120 Datalogger for Sampling Rates of 1, 20, and 100 Samples/sec (sps)

Digitizer	Sensitivity (counts/V)	rms Full Scale (counts)	SNR (dB)		
			1 sps	20 sps	100 sps
CH 6	408,655	5,779,268	144.2	143.0	140.5
CH 7	415,155	5,871,193	145.1	143.9	141.0
CH 8	407,468	5,762,482	144.9	143.6	141.3

The dynamic range is calculated by applying equation (3) on a time series of 24 hr which was recorded with short-circuited (50-ohm) input connectors. The noise rms is calculated between 0.01 Hz and 80% of the Nyquist frequency. The full-scale rms follows from the sensitivity values provided by the manufacturer (Quanterra Inc.) and the full-scale input (40 V). CH = channel.

the dynamic range of the digitizers are given on the right axes and follow from equation (5). The results in Figure 2 show that for frequencies above (roughly) 1 Hz the dynamic range for the three digitizers corresponds within a few decibels with the values in Table 1.

The effect of using a real seismic broadband signal on the dynamic range is shown in Figure 3. The digitizer outputs (recordings from the vertical component of an STS-2 sensor) are processed by using equation (14) and the same window lengths as above. For the 100 samples/sec and 20 samples/sec data the noise PSD of the shorted input measurement and the common input test are shown in gray and black lines. Notice that only one digitizer is shown to see the difference. At both sampling rates there is significant increase in the self-noise level and hence no significant decrease of the dynamic range. Figure 4 shows the measured gain ratios between the digitizers in the Q4120 datalogger, smoothed over a tenth of a decade. Between 0.01 Hz and 8 Hz, using data sampled with 20 samples/sec, the smoothed ratios are within 1.6% (or 0.14 dB) of the values given by the manufacturer.

These procedures are also applied to a NARS datalogger. The result of the coherency analysis on 20 samples/sec data is presented for one digitizer in Figure 5. Over the entire frequency range (0.001–8 Hz) some additional self-noise is visible, which decreases the dynamic range by a few decibels. At higher frequencies (1–8 Hz) the dynamic range increases to about 127 dB at 20 samples/sec, corresponding to a 20.8 bits digitizer. The PSD level at lower frequencies shows a significant smaller slope as compared with the Q4120. For frequencies below 0.01 Hz the PSD level of the NARS datalogger is below the Q4120 PSD level.

### Digitizer Noise Models

The dynamic behavior of the digitizers (Figs. 2 and 3) shows that the representation of the dynamic range by a single number is adequate for higher frequencies (above a few hertz) but not for lower frequencies. Evidently, the effect of

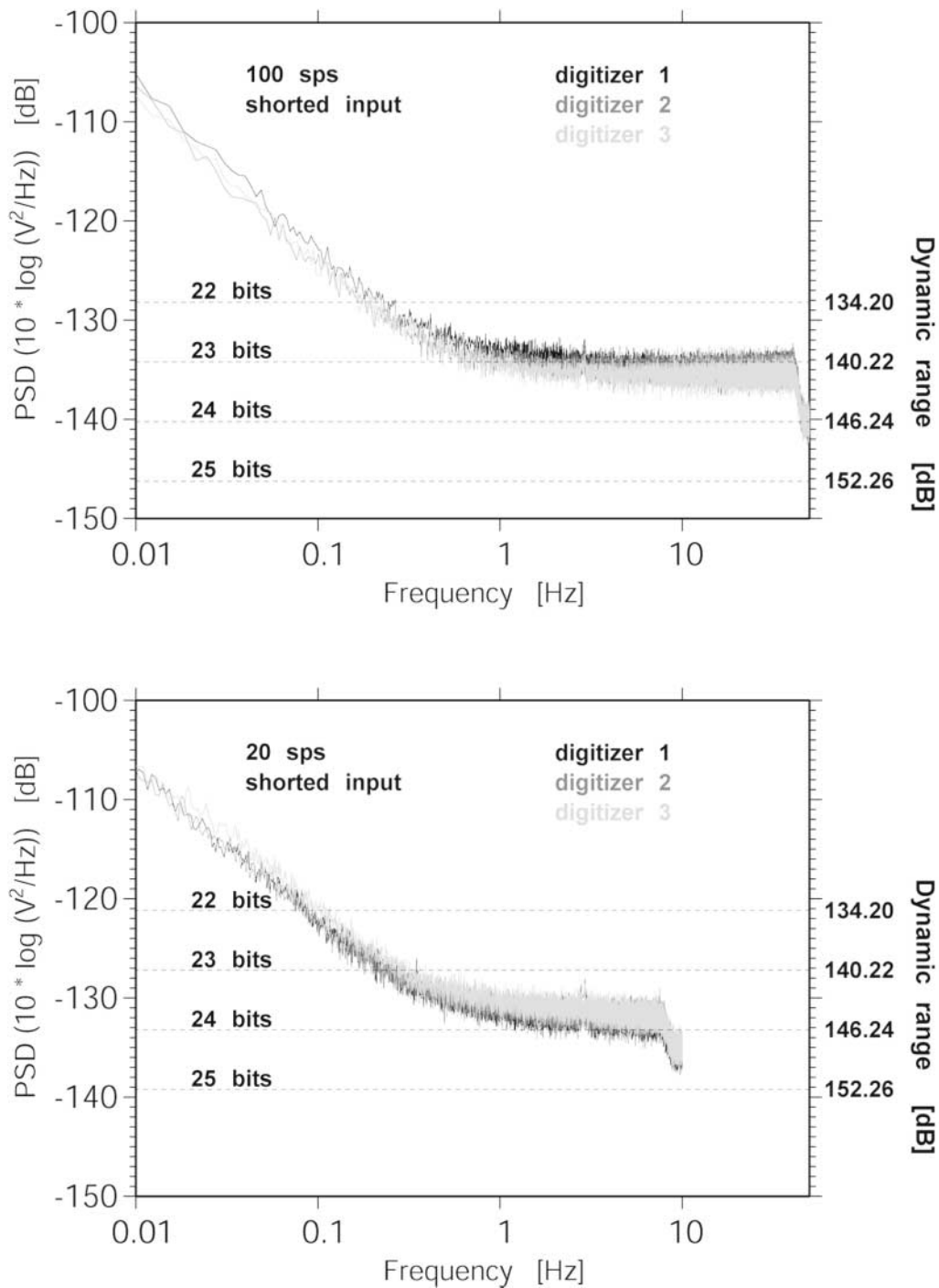


Figure 2. Noise floors (PSDs) for three digitizers in the Q4120 datalogger, using short-circuited (50-ohm) input recordings sampled with 100 samples/sec (top) and 20 samples/sec (bottom). The left axes represent the resolution (smallest input voltage that can be resolved) of the digitizer in decibels (relative to  $1 V^2/Hz$ ), the right axes show the corresponding dynamic range of the system, which has a full-scale (peak to peak) input of 40 V. The horizontal, dashed lines show the resolution of the digitizer in bits, which follows from equation (7). Notice the effect of the FIR filters beyond 80% of the Nyquist frequency.

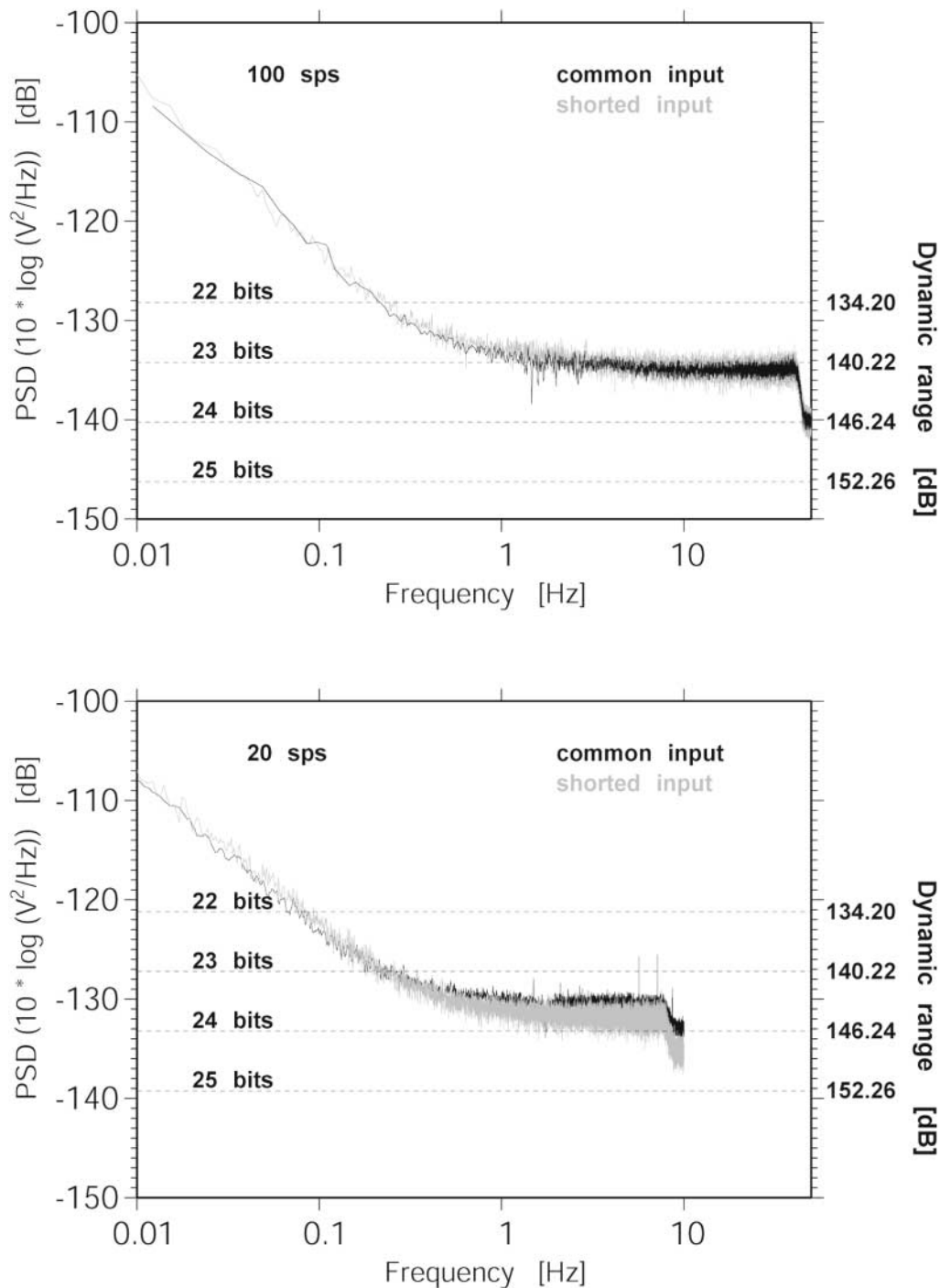


Figure 3. Self-noise floor (measured with common, vertical STS-2 signal, in black) for one digitizer in the Q4120 datalogger compared with the shorted-input self-noise (taken from Fig. 2, in gray), for 100 samples/sec (top) and 20 samples/sec (bottom).

the low-frequency behavior of the digitizer must be examined in studies where low-frequency information is extracted from the data, for example, in studies in seismic background noise (e.g., Stutzmann *et al.*, 2000; Vila and Macia, 2002), Earth's free oscillations studies (Suda *et al.*, 1998) or Earth tide studies. Simple models which describe the behavior of digitizers are useful in this respect.

The behavior of the Q4120 digitizer in Figure 3 at 20 samples/sec can be modeled by the superposition of white noise dominating at high frequencies and  $1/f$  type of noise dominating at low frequencies (Fig. 6). The model in this figure is based on equation (7) and represents a digitizer with a 23.6-bit broadband spectrum and a 24.7-bit spectrum with  $1/f^{1.55}$  noise:

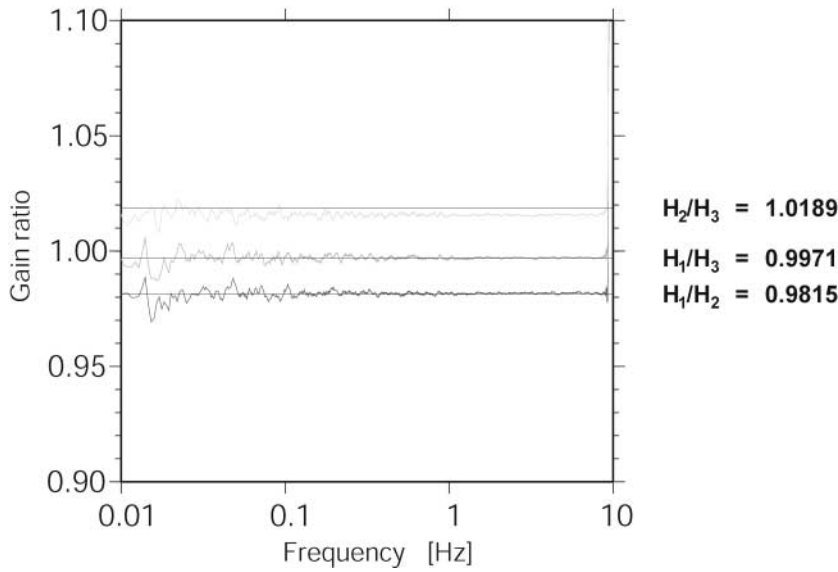


Figure 4. Measured gain ratios in the Q4120 datalogger using the 20 samples/sec recordings (common input), using equation (12). The ratios are smoothed over a tenth of a decade and compared with the ratios derived from the calibration sheet (black, horizontal lines).

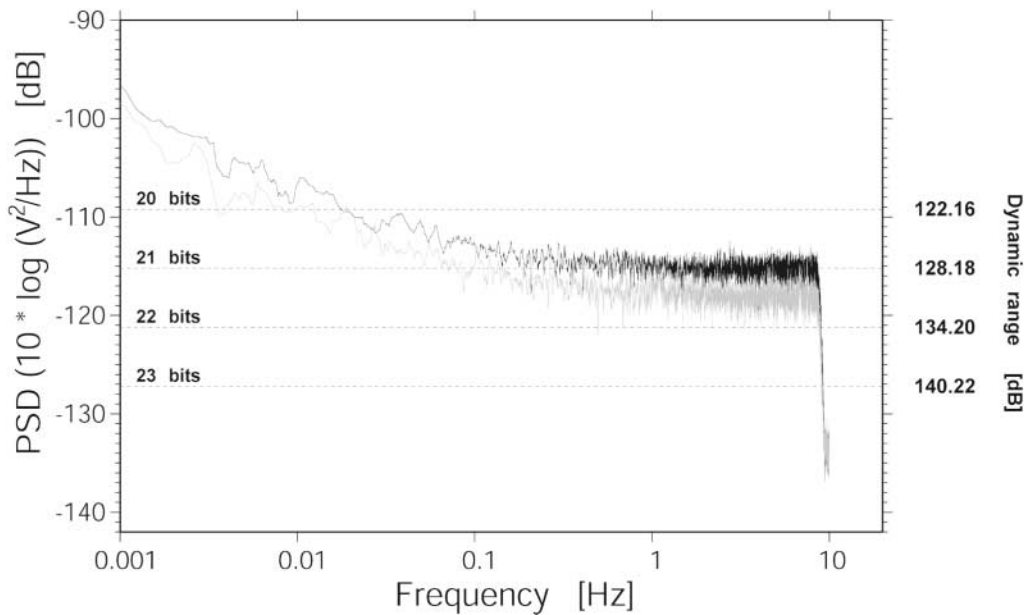


Figure 5. Observed digitizer noise in a NARS datalogger at 20 samples/sec. The light-gray noise level is observed using terminated inputs, the dark-gray noise level is observed while recording a broadband signal. The additional self-noise decreases the dynamic range by a few decibels.

$$\text{PSD}_{\text{Q4120}}(f) = 10 \cdot \log \left( \left( \frac{2A}{2^{23.6}} \right)^2 \cdot \frac{T}{6} + \left( \frac{2A}{2^{24.7}} \right)^2 \cdot \frac{T}{6} \cdot \frac{1}{f^{1.55}} \right) \quad (15)$$

(with  $T = 20$  samples/sec,  $2A = 40$  V). Clearly the noise of the digitizer falls in between pink noise ( $1/f$ ) and Brownian noise ( $1/f^2$ ). The interpretation for this behavior could be a series of different processes with  $1/f$  corner frequencies of electronic and thermal origin, that sum up to create an overall behavior as observed (J.M. Steim, personal comm., 2004).

The behavior of the NARS datalogger noise is modeled in Figure 7 by the same type of superposition as in equation (15): a 20.8-bit broadband spectrum dominating at high frequencies and a 23.0-bit spectrum with pink noise ( $1/f^{1.0}$ ) dominating at low frequencies:

$$\text{PSD}_{\text{NARS}}(f) = 10 \cdot \log \left( \left( \frac{2A}{2^{20.8}} \right)^2 \cdot \frac{T}{6} + \left( \frac{2A}{2^{23.0}} \right)^2 \cdot \frac{T}{6} \cdot \frac{1}{f^{1.0}} \right). \quad (16)$$

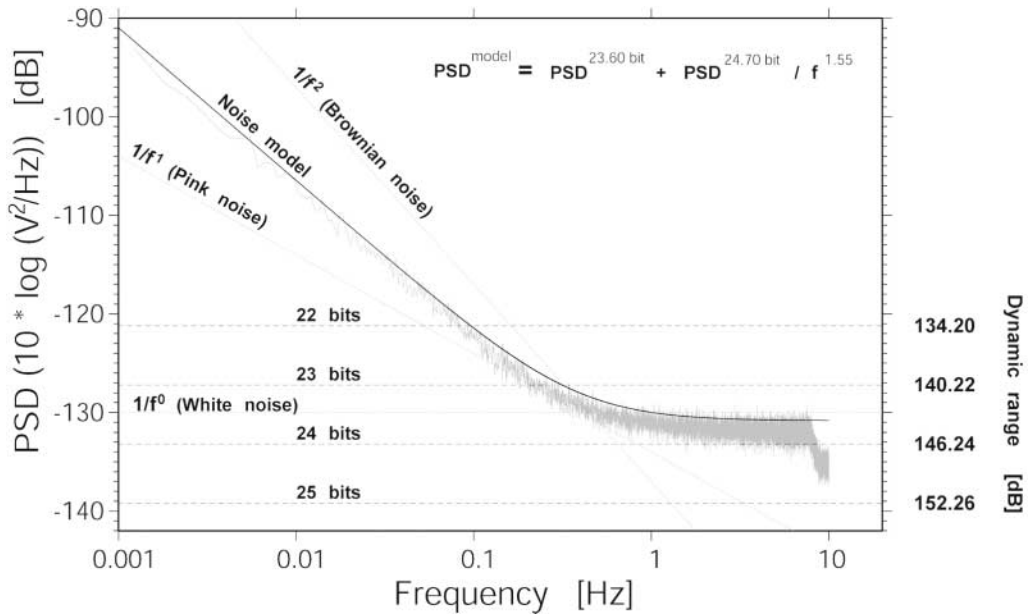


Figure 6. A behavioristic model of the digitizer noise in the Q4120 datalogger, based on the observed total noise floor in Figure 3 at a sampling rate of 20 samples/sec.

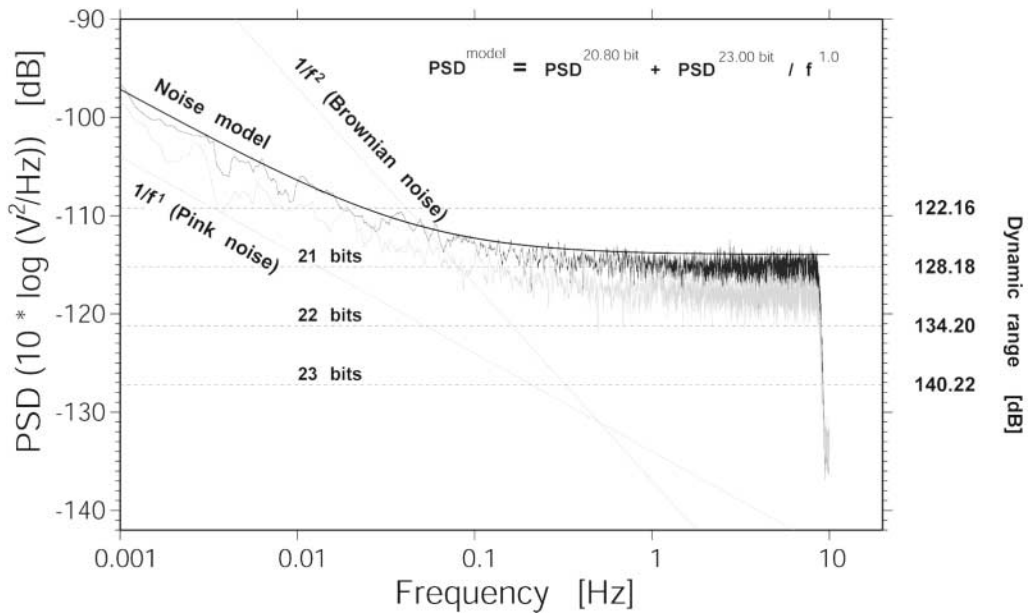


Figure 7. Observed and modeled digitizer noise in the NARS datalogger. The light- and dark-gray levels are taken from Figure 5. The behavioristic model is based on the observed self-noise level (dark-gray level) at a sampling rate of 20 samples/sec.

### Discussion

By analyzing the behavior of the digitizer it becomes possible to indicate for which frequencies the data can be biased by the digitizer. This is illustrated in Figure 8. This figure shows the convolution of the NLNM with (1) an ideal, noise-free sensor with a flat response and a gain of 1500 V/m/sec (2) a noise-free STS-1 (gain 2300 V/m/sec and corner frequency at 0.00277 Hz), and (3) a noise-free STS-2 (gain

1500 V/m/sec and corner frequency at 0.00833 Hz). These convolved NLNM levels are indicated as NL0, NL1, and NL2, respectively. Also the digitizer noise models (equations 15 and 16) are plotted in  $V^2/Hz$  by correcting the PSD models with the gain of the digitizer. The NARS datalogger noise crosses the noise levels (NL0, NL1, and NL2) at about 1 Hz and demonstrates that the interpretation of data in terms of seismic background noise must be done with care for

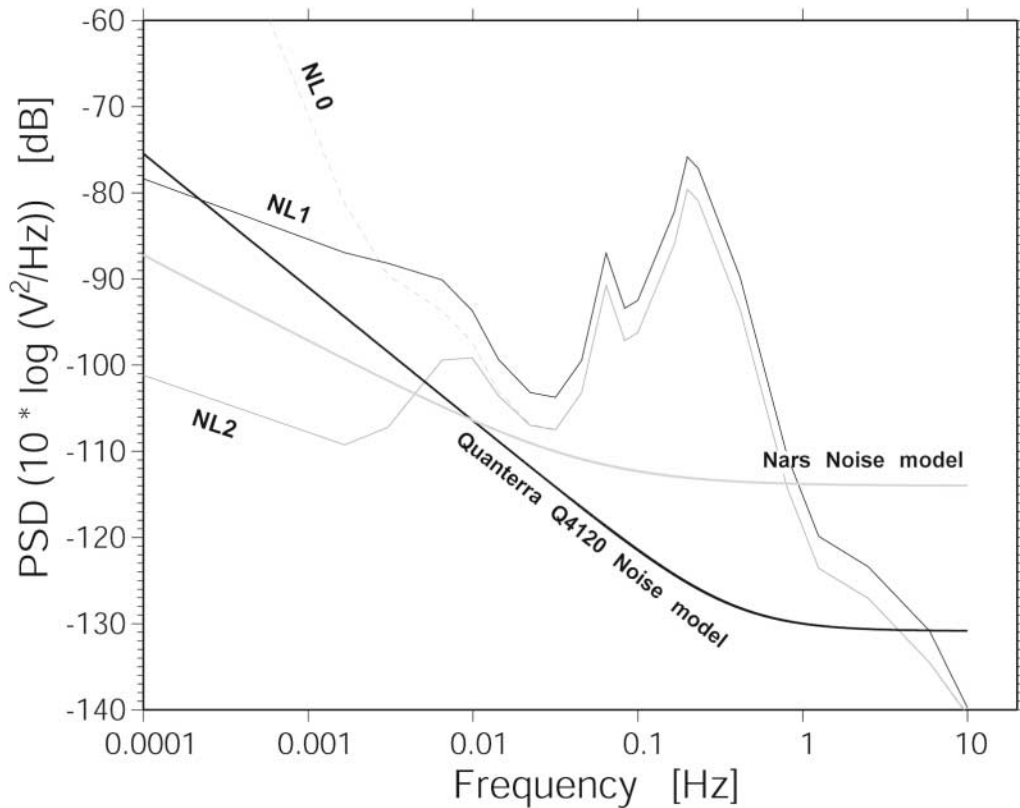


Figure 8. Digitizer models for the Q4120 and NARS dataloggers (at 20 samples/sec), compared with the NLNM convolved with a noise-free sensor with a flat velocity response and a gain of 1500 V/m/sec (NL0), a noise-free STS-1 sensor (NL1), and a noise-free STS-2 sensor (NL2). The PSDs are relative to  $1 \text{ V}^2/\text{Hz}$ . The figure visualizes for which frequencies the digitizer can be used without precaution.

frequencies above 1 Hz. The resolution of the datalogger would not be sufficient to record the seismic background noise at the quietest places in the world. For the Q4120 digitizer this upper limit is at about 8 Hz. Between 1 and 0.01 Hz the noise levels of both digitizers are well below levels NL0, NL1, and NL2, although there is a significant difference in their slope. Both digitizer noise levels dominate over NL2 at frequencies below approximately 0.007 Hz. So for frequencies below 0.007 Hz these digitizers can not record the NLNM using noise-free STS-2 sensors, simply because the  $1/f$  noise from the digitizer is dominating. Therefore, deconvolving this type of ideal data with the ideal sensor response would not resolve seismic background noise. For a noise-free STS-1 sensor this frequency boundary is at about 0.0002 Hz.

However, STS-1 and STS-2 sensors are not noise-free devices and, in fact, their self-noise is comparable to the Quanterra digitizer. It may therefore be difficult to separate the sensor noise and the digitizer noise in background noise recordings. As an example (Fig. 9) we have analyzed data from two systems at station HGN (Heimansgroeve, Netherlands): a shielded STS-2 (third generation; G. Streckeisen, personal comm., 2001) connected to a Q4120, and a STS-1 connected to a gain-ranged acquisition system (Dost and

Haak, 2002). Both systems are in the same vault at a distance of only 2 m. Data for the same period (2002) are deconvolved with the instrument response and shown in Figure 9 for three components. The horizontal noise (both components) is about 30–50 dB above the NLNM at frequencies below 0.01 Hz and is equally recorded by both systems. On the vertical component, however, a significant difference is visible below approximately 0.01 Hz. The background noise recorded by the STS-1 closely follows the NLNM, but the STS-2 recorded noise is 10–15 dB higher. Different noise sources may contribute to this difference, for example, barometric pressure fluctuations, variation in temperature, sensor noise, and digitizer noise. However, the effect of ground tilt and elastic response of the Earth due to atmospheric pressure fluctuations would be the same for the two instruments because they are on the same pier. This is confirmed by the similar, observed horizontal noise levels recorded by both instruments. A periodic deformation (at  $1.7 \times 10^{-3}$  Hz) of  $\pm 1 \mu\text{m}$  over a distance of 3 km, would result in horizontal noise which is about 40 dB above the vertical noise (Wielandt, 2002b). Local pressure variations in the vault may affect the seismometers in at least three ways (Wielandt, 2002b): (1) a buoyancy force when the sensor is not sealed, (2) adiabatic changes of temperature, and (3) deformation of

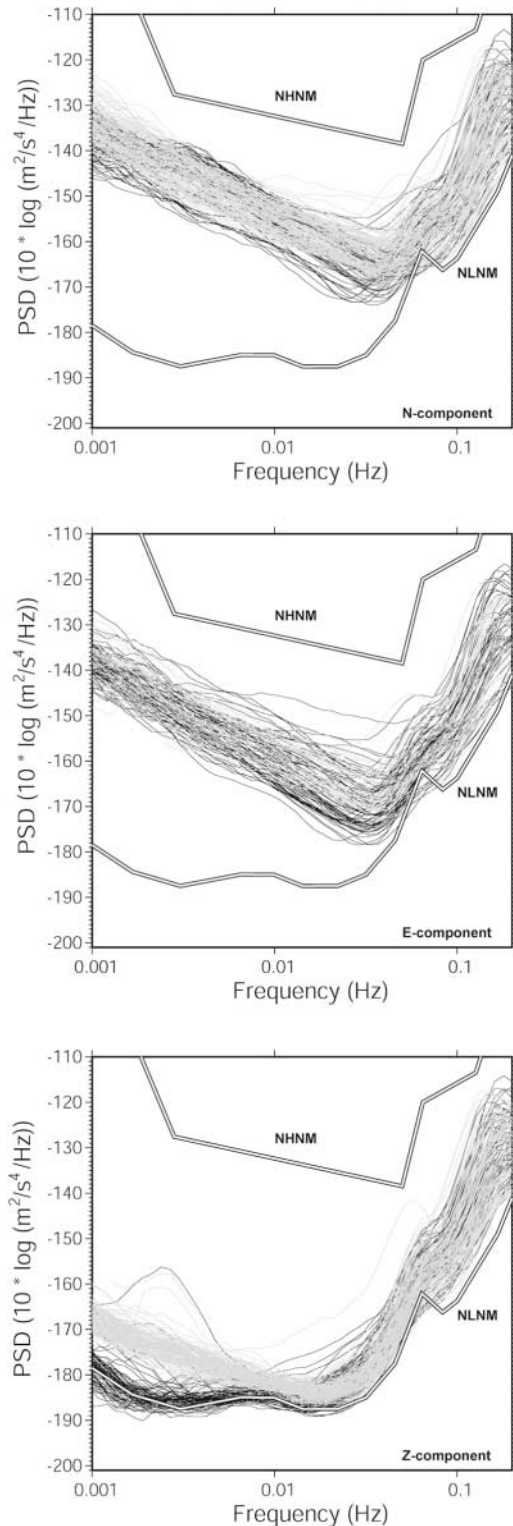


Figure 9. Seismic background noise recorded at station HGN by the STS-2 + Q4120 datalogger (gray) and the STS-1 + gain range datalogger (black). From top to bottom are shown the north-south (N), east-west (E), and vertical (Z) components. Each line represents an estimate of the background noise averaged over one day in 2002. All estimates are corrected for the instrument response.

the sensor housing. However, the casings of the STS-1 and STS-2 sensors are designed to suppress these kind of effects. Also the sensors are thermally insulated; the STS-2 is covered with fiber wool and a heat-reflecting blanket, all covered by a stainless steel jacket, and the STS-1 instrument is covered by a partially evacuated glass bell. Consequently, we assume that the temperature effect for the frequencies between 0.001 and 0.01 Hz does not have a great impact on the noise level. Another reason for the discrepancy between the STS-1 and STS-2 vertical-component observations in Figure 9 could be related to deviations between the measured and the manufacturers “nominal” response. Fels and Berger (1994) measured response deviations for a STS-1 of up to 1% in amplitude and  $1^\circ$  in phase between 0.2 and 100 mHz, and up to 12% in amplitude and  $5^\circ$  in phase for frequencies above 5 Hz. These deviations, however, are too small to explain the difference of 10–15 dB. This is also confirmed by the observation that the horizontal components do not show such a significant difference.

The previously modeled digitizer noise (equation 15) is useful here because it excludes the digitizer as origin of the observed difference in noise level. Between 0.01 and 0.001 Hz the digitizer model is about 10 dB lower than the NLNM and could therefore not contribute to this difference. Given these observations and assumptions the discrepancy in noise level seems to be caused by the sensor noise level, although this seems in contradiction with the noise level presented in the STS-2 manual (Streckeisen, 1991). To validate this explanation we compared the observations with the noise model of the STS-2 by Wielandt and Widmer-Schmidrig (2002) in Figures 10 and 11. Figure 10 compares the NLNM, the STS-2 noise model, and the digitizer model. Figure 11 compares the STS-2 noise model with the STS-1 and STS-2 observations at HGN. The noise model fits very well with the STS-2 observations because it marks within a few decibels the lower boundary of the STS-2 observations. Also the slope of the  $1/f$  noise model fits very well the observations. However, recent studies by Widmer-Schmidrig (2003) and Berger *et al.* (2004), respectively, show smaller (5–6 dB) and larger (19–24 dB) differences between vertical STS-1 and STS-2 noise levels for frequencies between 1 and 2 mHz. Several factors may contribute to the differences, such as the quality of installation of seismometers, the variable quality among the different STS-2 sensors, or differences in self-noise between STS-2 sensors. Our new technique will be ideal to measure the self-noise of STS-2 (and other) sensors by placing three sensors together at the same location. Differences in quality between sensors and self-noise, or inaccurate knowledge of transfer functions, will not bias the measurement of the self-noise.

## Conclusions

The self-noise of a digitizer as function of the frequency is important information that has to be considered during the interpretation of data. We developed a new method to esti-

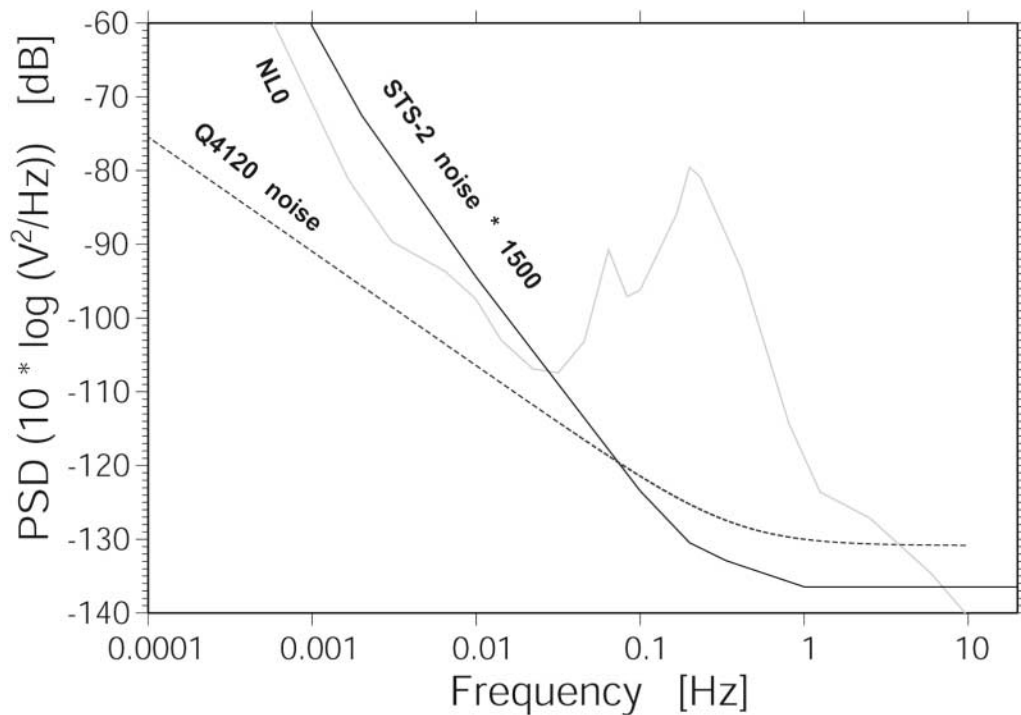


Figure 10. STS-2 noise (Wielandt and Widmer-Schnidrig, 2002) compared with the Q4120 noise and NL0 (see Fig. 8), by showing the corresponding PSDs relative to  $1 \text{ V}^2/\text{Hz}$ . For this purpose the STS-2 model is multiplied by 1500.

mate instrumental noise in a three-channel, linear system based on analysis of the output recordings only. The technique can be applied to any datalogger or sensor in normal field operation conditions. We applied the technique to a Q4120 datalogger and a NARS datalogger and modeled the behavior of the self-noise level by only a few parameters describing resolution and  $1/f$  noise. The two dataloggers tested here show significant differences in these parameters: at higher frequencies (above a few hertz) the resolution for the Q4120 at 20 samples/sec is 23.8 bites, and 20.6 bits for the NARS; the slope of the  $1/f$  noise is 1.55 for the Q4120 and 1.00 for the NARS. Also, the NARS datalogger showed some additional self-noise, which is negligible in the Q4120. The usefulness of such models was shown in the interpretation of seismic background noise recorded at station HGN by an STS-1 and a STS-2. The digitizer model excludes the digitizer noise to contribute to this difference. The difference in noise levels between those two instruments between 0.01 and 0.001 Hz is in agreement with Wielandt and Widmer-Schnidrig (2002).

### Acknowledgments

We thank Erhard Wielandt for his enthusiastic and constructive comments on this manuscript and the new technique in particular. Also the suggestions and comments by R. Widmer-Schnidrig helped us to improve the manuscript. All figures were generated using the software package GMT (Wessel and Smith, 1991).

### References

- Aki, K., and P. G. Richards (1980). *Quantitative Seismology*, W. H. Freeman, San Francisco.
- Baker, C. B. (1997). How to get 23 bits of effective resolution from your 24-bit converter, *Burr-Brown Application Bulletin*, AB-120, Tucson, Arizona.
- Beauduin, R., P. Lognonne, J. P. Montagner, S. Cacho, J. F. Karczewski, and M. Morand (1996). The effects of the atmospheric pressure changes on seismic signals or how to improve the quality of a station, *Bull. Seism. Soc. Am.* **90**, no. 4, 952–963.
- Bennett, W. R. (1948). Spectra of quantized signals, *Bell System Tec. J.* **27**, 446–472.
- Berger, J., D. C. Agnew, R. L. Parker, and W. E. Farrell (1979). Seismic system calibration: 2. Cross-spectral calibration using random binary signals, *Bull. Seism. Soc. Am.* **69**, no. 1, 271–288.
- Berger, J., P. Davis, and G. Ekström (2004). Ambient Earth noise: a survey of the global seismographic network, *J. Geophys. Res.* **109**, B11307.
- Candy, C. J., and G. C. Temes (1992). Oversampling methods for A/D and D/A conversion, *Oversampling Delta-Sigma Delta Converters*, C. J. Candy and G. C. Temes (Editors), IEEE Press, Piscataway, New Jersey.
- Clinton, J. F., and T. H. Heaton (2002). Performance of the VSE-355G2 strong-motion velocity seismometer, Report to the IRIS-GSN subcommittee, California Institute of Technology.
- Dost, B., and H. W. Haak (2002). A comprehensive description of the KNMI seismological instrumentation, *Technical Report, TR-245*, Koninklijk Nederlands Meteorologisch Instituut, De Bilt, Netherlands.
- Fels, J.-F., and J. Berger (1994). Parametric analysis and calibration of the STS-1 seismometer of the IRIS/IDA seismographic network, *Bull. Seism. Soc. Am.* **84**, no. 5, 1580–1592.
- Freybourger, M., J. Hinderer, and J. Trampert (1997). Comparative study

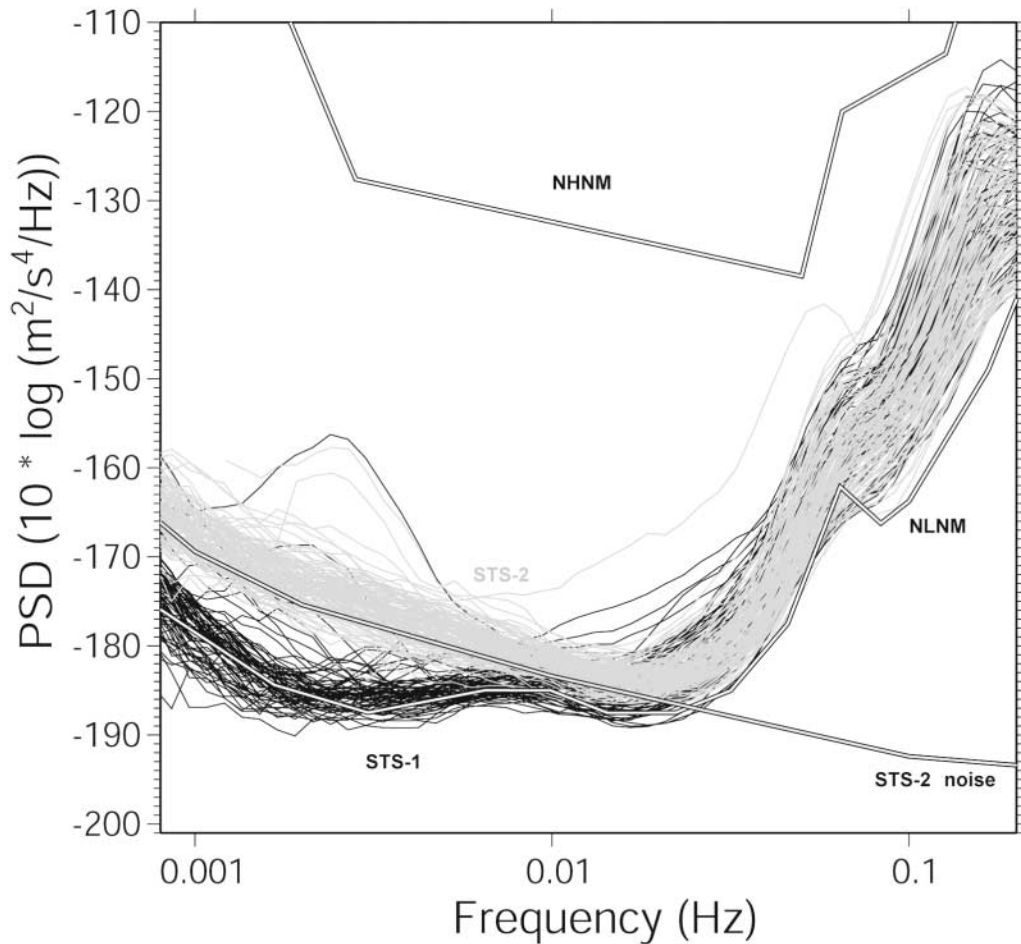


Figure 11. PSDs of seismic background noise levels at station HGN in 2002 observed by the vertical component of the STS-1 and a STS-2 sensor, compared with the STS-2 noise model from Wielandt and Widmer-Schmidrig (2002).

- of superconducting gravimeters and broadband seismometers STS-1/Z in seismic and subseismic frequency bands, *Phys. Earth Planet. Interiors* **101**, 203–217.
- Gray, R. M. (1990). Quantization noise spectra, *IEEE Trans. Inf. Theory* **36**, no. 6, 1220–1244.
- Holcomb, L. G. (1989). A direct method for calculating instrument noise levels in side-by-side seismometer evaluations, *U.S. Geol. Surv. Open-File Rept.* 89-214.
- Holcomb, L. G. (1990). A numerical study of some potential sources of error in side-by-side seismometer evaluations, *U.S. Geol. Surv. Open-File Rept.* 90-406.
- Hutt, C. R. (1990). *Standards for Seismometer Testing—A Progress Report*, U.S. Geological Survey, Albuquerque Seismological Laboratory, Albuquerque, New Mexico.
- IRIS (2003). Global Seismograph Network Data Logger Specifications, Incorporated Research Institutions for Seismology, 1200 New York Avenue, Washington, D.C. 20005.
- McDonald, T. S. (1994). Modified noise power ratio testing of high resolution digitizers, Sandia National Laboratories Report, 94-0221.
- Oppenheim, A. V., and R. W. Schaffer (1998). *Discrete-Time Signal Processing*, Prentice Hall, New York.
- Pavlis, G. L., and F. L. Vernon (1994). Calibration of seismometers using ground noise, *Bull. Seism. Soc. Am.* **84**, no. 4, 1243–1255.
- Peterson, J. (1993). Observations and modeling of seismic background noise, *U.S. Geol. Surv. Open-File Rept.* 93-322, 95 pp.
- Press, W. H., B. P. Flannery, S. A. Teukolsky, and W. T. Vetterling (1988). *Numerical Recipes in C*, Cambridge University Press, New York.
- Rosat, S., J. Hinderer, D. Crossley, and L. Rivera (2003). The search for the Slichter mode: comparison of noise levels of superconducting gravimeters and investigation of a stacking method, *Phys. Earth Planet. Interiors* **140**, 183–202.
- Roult, G., and W. Crawford (2000). Analysis of ‘background’ free oscillations and how to improve resolution by subtracting the atmospheric pressure signal, *Phys. Earth Planet. Interiors* **121**, 325–338.
- Steim, J. M. (1986). The very-broad-band seismograph, *Ph.D. thesis*, Harvard University, Cambridge, Massachusetts, 184 pp.
- Streckeisen, G. (1991). STS-2 manual, CH-8422, Pfungeu, Switzerland.
- Stutzmann, E., G. Roult, and L. Astiz (2000). GEOSCOPE station noise levels, *Bull. Seism. Soc. Am.* **90**, no. 3, 690–701.
- Suda, N., K. Nawa, and Y. Fukao (1998). Earth’s background free oscillations, *Science* **279**, 2089–2091.
- Vila, J., and R. Macia (2002). The broadband seismic station CADI (Tunel del Cadi, Eastern Pyrenees), part II: long-period variations of background noise, *Bull. Seism. Soc. Am.* **92**, **8**, 3329–3334.
- Warburton, W. (2004). Potential of a superconducting long-period seismometer, IRIS Broad-band Seismometer Workshop, 24–26 March 2004, Lake Tahoe, California.
- Welch, P. D. (1967). The use of fast fourier transform for the estimation of power spectra: a method based on time averaging over short, modified periodograms, *IEEE Trans. Audio Electroacoust.* AU-15, 70–73.

- Wessel, P., and H. F. Smith (1991). Free software helps map and display data, *EOS* **72**, 441.
- Widmer-Schmidrig, R. (2003). What can superconducting gravimeters contribute to normal-mode seismology? *Bull. Seism. Soc. Am.* **93**, no. 3, 1370–1380.
- Wielandt, E. (2002a). Seismometry, in *International Handbook of Earthquake and Engineering Seismology, Part A*, W. H. K. Lee, H. Kanamori, P. C. Jennings, and C. Kisslinger (Editors), Academic Press, San Diego, California, 283–304.
- Wielandt, E. (2002b). Seismic sensors and their calibration, in *IASPEI—New Manual of Seismological Observatory Practice*, P. Bormann (Editor), GeoForschungsZentrum Potsdam, Potsdam, Germany.
- Wielandt, E., and J. M. Steim (1986). A digital very-broad-band seismograph, *Ann. Geophys.* **4**, B, no. 3, 227–232.
- Wielandt, E., and R. Widmer-Schmidrig (2002). Seismic sensing and seismic noise, in *Ten Years of German Regional Seismic Network (GRSN)*, Report 25 of the Senate Commission for Geosciences, M. Korn (Editor), Wiley-VCH Verlag GmbH, Weinheim, Germany.
- Zürn, W., and R. Widmer (1995). On noise reduction in vertical seismic records below 2 mHz using local barometric pressure, *Geophys. Res. Lett.* **22**, no. 24, 3537–3450.

Royal Netherlands Meteorological Institute (KNMI)  
Seismology Division  
Wilhelminalaan 10  
3732 GK, De Bilt, Netherlands  
sleeman@knmi.nl  
(R.S.)

University of Utrecht  
Faculty of Geosciences  
Budapestlaan 4  
3584 CD, Utrecht, Netherlands  
wettum@geo.uu.nl  
jeannot@geo.uu.nl  
(A.V.W., J.T.)

Manuscript received 23 February 2005.